



Stress-dependent anisotropy and fluid content identification in transversely isotropic rocks: theoretical predictions versus laboratory measurements

Hengxin Li ^a, Guangzhi Zhang ^{a, b}, Jiajia Zhang ^a, Lanhua Huang ^a

^a School of Geosciences, China University of Petroleum (East China)

^b Laboratory for Marine Mineral Resources, Qingdao National Laboratory for Marine Science and Technology

Contact email: s17010122@s.upc.edu.cn

Introduction

Characterization of stress-dependent anisotropy and identification of fluid content have been two important tasks for shale reservoir prediction. In this paper, we present a new indicator of fluid content in cracks for a general transversely isotropic distribution of micro cracks. A dimensionless fourth-rank tensor is presented, which is sensitive to fluid content and the orientation distribution of cracks. We apply the porosity-deformation approach to ultrasonic measurements on the Jurassic North Sea shale (Hornby, 1998) and predict the changes of crack density tensors, the new indicator of fluid content, as well as the number of cracks in different directions with increasing pressure.

Methodology

In the case of transversely isotropic symmetry, x_3 is the axis of symmetry with (x_1, x_2) being the horizontal bedding plane. Second-rank and fourth-rank crack density tensors α_{ij} and β_{ijkl} are expressed in terms of the extra compliance tensor ΔS_{ij} (Sarout et al., 2007). For a general anisotropic distribution of micro cracks, we introduce a new indicator of fluid content:

$$\left(\frac{B_N}{B_T} \right)_{ani} = \sum_{i=1}^3 \left(\frac{B_N}{B_T} \right)_i w_i \quad (1)$$

Where $(B_N/B_T)_i$ represents the indicator of fluid content along x_i -axis ($i=1, 2, 3$), which can be derived from these crack density tensors α_{ij} and β_{ijkl} ; w_i is the volume fraction of cracks normal to the x_i -axis. In analogy to the normalized second-rank tensor α_{ij} , we define a dimensionless fourth-rank tensor H_{ijkl} :

$$H_{ijkl} = \frac{3E(v-2)}{16(1-v^2)v} \beta_{ijkl} = \frac{\psi a^3}{V} \sum_r n_i^{(r)} n_j^{(r)} n_k^{(r)} n_l^{(r)} \quad (2)$$

The parameter ψ strongly depends on the fluid content and depends much less on the pore geometry. And we assume the pore aspect ratio is identical for all cracks.

Results

The predicted crack density tensors show good agreement with corresponding measurements. The sample is in the saturated state, the fourth-rank tensor components are on the same order of magnitude but slightly lower than the values of α_{ij} . α_{ij} and β_{ijkl} are of opposite signs over most of the stress range, which implies that the discontinuities are more compliant in shear than in compression (Figure 1a). N_{33} is larger than N_{11} , which indicates that there are more horizontally oriented micro cracks than vertically oriented. It is also observed that N_{11} and N_{33} gradually tends to zero as confining pressure increases, which means that crack-like pores are closed completely at the high confining pressure (Figure 1b).

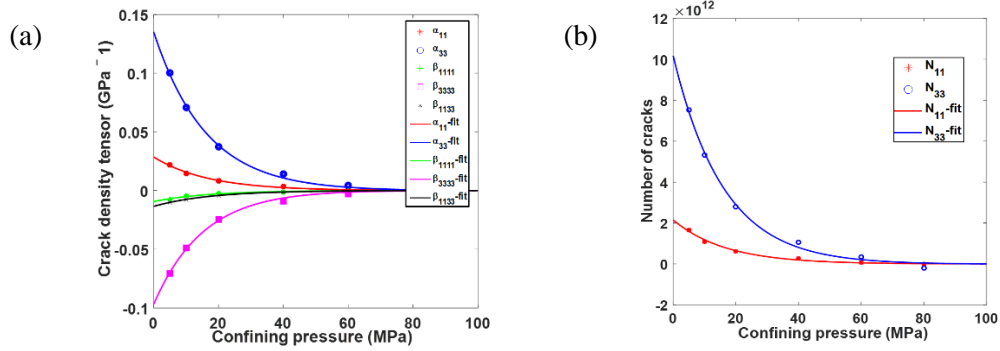


Figure 1: Measured (symbols) and theoretically predicted (lines) (a) crack density tensors and (b) number of cracks variation with confining pressure.

We observe good agreement between the theoretically predicted indicator of fluid content and the calculated values obtained from measurements. It is seen that $(B_N/B_T)_1$ and $(B_N/B_T)_3$ are shown to bear a contrary pressure dependency. The ratio $(B_N/B_T)_{ani}$ for fully saturated samples can show a lower value compared with measurements on air-dry shales. The dimensionless fourth-rank tensor H_{ijkl} obtained from porosity-deformation approach is well agree with the measurements. The components of H_{ijkl} decrease as the magnitude of the confining pressure increases, which is consistent with the continuous closure of those micro-cracks and grain boundaries throughout the experiment. The important observation is that the values of H_{ijkl} provide insight into the saturation state of the shale, since the values of H_{ijkl} in the saturated state are almost one order of magnitude larger than that in the dry case.

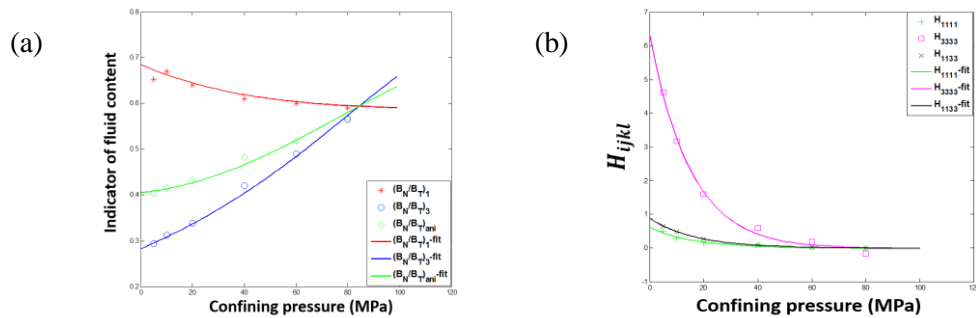


Figure 2: Evolution of the (a) indicator of fluid content and (b) the dimensionless fourth-rank tensor H_{ijkl} under confining pressure.

Conclusions

The new indicator of fluid content and the dimensionless fourth-rank tensor are found to be sensitive to the saturation state of the shale. The elastic wave anisotropy can be explained by the crack density anisotropy, since there is a significant difference between the vertical and the horizontal crack density.

Acknowledgements

We would like to acknowledge the sponsorship of the National Natural Science Foundation of China (41674130), the National Oil and Gas Major Projects of China (2016ZX05027004-001).

References

- [1] Hall S A, Kendall J-M, Maddock J, Fisher Q. 2008. Crack density tensor inversion for analysis of changes in rock frame architecture. *Geophys J Int*, 173: 577-592.
- [2] Ciz R, Shapiro S A. 2009. Stress-dependent anisotropy in transversely isotropic rocks: Comparison between theory and laboratory experiment on shale. *Geophysics*, 74: D7-D12.